ZORICA MOJOVIĆ[1]
LJILJANA ROŽIĆ[1]
TATJANA NOVAKOVIĆ[1]
ZORICA VUKOVIĆ[1]
SRDJAN PETROVIĆ[1]
DANIJELA RANĐELOVIĆ[2]
MIODRAG MITRIĆ[3]

[1]IChTM - Department of Catalysis
and Chemical Engineering, Uni-
versity of Belgrade, Belgrade,
Serbia
[2]IChTM - Department of Microelec-
tronic Technologies and Single
Crystals, University of Belgrade,
Belgrade, Serbia
[3]Condensed Matter Physics
Laboratory, Vinča Institute,
University of Belgrade, Belgrade,
Serbia

ELECTROCHEMICAL BEHAVIOR OF $H_3PW_{12}O_{40}$/ACID-ACTIVATED BENTONITE POWDERS

Electrochemical behavior of 12-tungstophosphoric acid (HPW)/acid-activated bentonite (AAB) powders with various loadings of HPW was investigated. The physicochemical properties of the prepared powders were examined by X-ray powder diffraction, nitrogen adsorption-desorption isotherms, atomic force microscopy and cyclic voltammetry measurements. The results indicated that the prepared powders are composed mainly of oriented domains of large rock blocks, probably resulting from a preferable deposition of bentonite particles having a face-to-face interaction. The particles had a mainly disordered mesoporous structure with a pore volume that varied according to the pore size in the range of 2-50 nm. In addition, the particles had crystallite size between 4.9 and 9.0 nm. The electrocatalytic activities of prepared HPW/AAB electrodes were studied in the oxidation of NO_2^- and the results revealed that the electrodes possessed relatively higher nitrite oxidation currents than AAB electrode. The best electroactivity was observed for HPW3/AAB electrode (AAB + + 20 wt.% HPW) and the limit of detection (3σ) was determined as 8 μM.

Keywords: bentonite modified electrode, phosphotungstic acid, oxidetion of nitrites, cyclic voltammetry.

Bentonites are widely used in a range of applications because of their high cations exchange capacity, swelling capacity, porosity, high surface areas and consequential strong adsorption and absorption capacities. Treatment of catalytic supports and adsorbents and the effect of acid attack on properties such as surface area, acidity and bleaching efficiency has received considerable attention [1-4] bentonites with mineral acids is a common way to modify the above properties and impart acidity to the clay surface [5-8]. Acid-activated bentonite powders have been used in diverse applications such as adsorbent, catalysts and bleaching earth [9]. Also, acid-activated bentonites are a practical and promising solid electrolyte material. It has been employed as a useful modified electrode material in recent years [6,10,11]. Most investi-

gations fall into two main categories: the exploitation of electrochemistry to characterize transport issues of various substances in bentonite by means of the voltammetry response of electroactivity probes located within the layered structure and the design of electrochemical sensors by exploiting the combination of bentonite properties with selected redox processes. The second category concerns mainly the electrochemical quantification of various inorganic ions or organic species at trace levels subsequent to preconcentration in the bentonite powders. Bentonites are also good candidates to support biomolecules or electrocatalysts that are often employed to modify electrode surfaces for electro analysis purposes [12]. Therefore, immobilization of heteropoly acid (HPA) on support simplifies their electrochemical study and facilitates their applications [13]. Heteropolyanions have ability to accept various numbers of electrons giving rise to mixed-valency species, which has made these compounds very attractive in electrode modification and electrocatalytic research [14]. HPA supported in a different manner has been used as ascorbic acid sensor

[15], nitrite sensor [16-21], for the oxygen reduction reaction [22]. The cyclic voltammetry (CV) studies demonstrated that electrode containing HPA has high stability, fast response and good electrocatalytic activity for the reduction of nitrite [23].

In this study, electrochemical behavior of the acid-activated bentonite powder with various loading of HPW was investigated. An attempt was made to correlate the electrochemical properties with the structural and chemical features of the modifying bentonite powders. Moreover, possible applications of HPW/AAB electrodes as nitrite sensor were studied.

MATERIAL AND METHODS

The results of our previous investigations on the modeling and optimization of bentonite powder (from south Serbia) activation via response surface methodology [8] were applied to modified bentonite, which was used as a starting material (sample AAB) in the current study. Chemical activation of bentonite powder was carried out in glass reactor at 90 °C, during 3 h with solid-liquid ratio 1:4.5, with HCl concentration of 4.5 M. Acid-activated bentonite powder obtained under optimal conditions possessed the following chemical composition (wt.%): SiO_2 = 73.66, Al_2O_3 = 12.28, Fe_2O_3 = 4.73, CaO = 0.70, MgO = 1.99, Na_2O = 0.60, K_2O = 0.30, TiO_2 = 0.57, and ignition on loss 5.17.

12-Tungstophosphoric acid (HPW) modified acid-activated bentonite powder was prepared according to the method described in the literature [24]. HPW was dissolved in methanol, and the resulting solution was added slowly to 5, 10 and 20 wt.% of acid activated bentonite powder, assigned as HPW1/AAB, HPW2/AAB and HPW3/AAB, respectively. To remove residual methanol, wet samples were dried in a water bath, and further dried in an oven for 2 h at 100 °C. The sample was stored in a sealed bottle until use.

The crystallinity of the samples was determined by powder X-ray diffraction (XRD) on a Philips PW 1710 with CuK. radiation (40 kV, 30mA, λ = 0.154178 nm) at a 2θ scan range of 3-70°.

The specific surface area and the pore volumes were determined *via* N_2 adsorption-desorption isotherms, which were obtained at 77 K with an automatic adsorption apparatus (Sorptomatic 1990 Thermo Finningen). The adsorption data were used to calculate the values of the specific surface area, *S*, from the monolayer capacity, N_m. The latter quantity was evaluated from the linearized BET adsorption isotherm equation [25]:

$$\frac{1}{N(X-1)} = \frac{C_{BET}-1}{C_{BET}N_m}X + \frac{1}{C_{BET}N_m} \tag{1}$$

where X= p/p_0, monolayer capacity, N_m and the so-called BET constant, C_{BET}. The pore size distribution was calculated according to the Barret-Joyner-Halenda method using the N_2 desorption isotherms [26]. In order to discriminate between the external plus mesoporous surface area and the micropore volume we made use of the α_s plot method [27]. The α_s plots, defined as α_s = $(n/n_s)_{ref}$ where n_s and *n* are the amounts of N_2 adsorbed by the reference solid at $p/p_0 \neq$ ≠ *s* and p/p_0 = *s*, respectively, provide to be as a very valuable tool to investigate the porosity of solid. By plotting for a test sample the nitrogen volume, *V*, adsorbed at a relative pressure, p/p_0, as a function of the α_s value from the reference material at the corresponding p/p_0, valuable information can be obtained about the porous structure of the solids.

The morphological characteristics of the samples were investigated *via* atomic force microscopy (AutoProbe CP-Research SPM, TM Microscopes - Veeco) using 90 μm large area scanners. Measurements were carried out in air using non-contact AFM mode. Veeco phosphorus (*n*) doped silicon Tap300 metrology probes, model MPP-11123-10 with Al reflective coating and symmetric tip were used. Nominal width, length and thickness of these rectangular shaped cantilevers are 35, 125 and 4 μm, respectively. Nominal thickness of the aluminum reflective coating on the backside of the cantilever is 40 nm. Front side of the cantilever is not coated, nominal force constant of used cantilevers is 40 N/m and resonance frequency is in the range (200-400) kHz. During the measurements driving frequency of the cantilever vibrations was around 300 kHz. 2D and 3D AFM images were created and analyzed using two software packages, Image Processing and Data Analysis, version 2.1.15, and SPMLab Analysis software, VEECO DI SPMLab NT Ver. 6.0.2.

In order to use the HPW/AAB powder as electrode materials, the samples were homogeneously dispersed in 5 mass% Nafion solutions in mixture of isopropyl alcohol and water using ultrasonic bath. The electronic conductivity of the samples was enhanced by adding 10 mass% of carbon black Vulcan XC72 (Cabot Corp.) into the initial suspension. Droplets (10 μl) of these suspensions were placed on the surface of a glassy carbon rotating disc electrode. Diameter of glassy carbon electrode was 0.2 cm. After the solvent removal by evaporation at 90 °C, the samples particles were uniformly distributed on the glassy carbon support in a form of thin layer [27]. For the electrochemical investigations in a three-electrode glass cell, as a working electrode was used a glassy carbon rotating disc electrode covered with a layer of homogeneous mixture containing carbon black combined with each of the following bentonite based samples

separately. The reference electrode was Ag/AgCl in 1M KCl, while a platinum foil served as a counter electrode. The oxidation of NO_2^- in 1 mM HCl + 1 M NaCl solution containing different concentrations of $NaNO_2$ was investigated. The device used for the electrochemical measurements was 757 VA Compu-trace Metrohm. The cyclic voltammetry and square wave voltammetry methods were employed. The cyclic voltammograms (CV) were recorded at polarization rate of 10 mV s⁻¹ and rotation rate of 600 rpm, unless otherwise stated.

The square wave voltammograms (SWV) were recorded in potential window of 0.5 to 1 V *vs*. Ag/AgCl electrode with following parameters: pulse amplitude 50 mV, scan increment 10 mV and frequency 1 Hz. A blank square wave voltammogram was recorded in 10mL of supporting electrolyte. The definite aliquot of 0.5 M $NaNO_2$ stock solution was added to the beaker, stirred vigorously to ensure thorough mixing, and another square wave voltammogram was recorded. This procedure was repeated for the same concentration range as when CV was employed.

RESULTS AND DISCUSSION

Physical characterization

Prior to the electrocatalytic studies, the purity and mesoporous structure of the bentonite powders were evaluated. Figure 1 shows the X-ray powder diffraction patterns of acid-activated bentonite (AAB) and bentonite powders with HPW loadings of 5, 10 or 20% (HPW1/AAB, HPW2/AAB and HPW3/AAB, respectively), exhibiting a first order peak in the region of $2\theta <$ < 10° and revealing the main particle size differences between the AAB and the HPW/AAB samples.

The (001) reflection corresponds to the basal spacing of the beidellite, are in good agreement with previously reported values [28]. However, HPW/AAB samples show a small shift of the main reflection (001) which indicates that HPW was in an amorphous state and was randomly distributed on the bentonite surface or incorporated in the pores of the bentonite. The full width at half maximum (FWHM) of the main reflection peak can be used to determined the crystallite size of the bentonite particles, according to Scherer's equation.

The calculated results (Table 1) indicated that the sample HPW3/AAB possess minimum value of crystallite size, which might provide good electrochemical behavior of modified electrode.

It is possible to investigate the porosity of the AAB and HPW/AAB powders by transforming the isotherm data in the form of the α_s plots. V_{ads}-α_s plots of all samples are shown in Figure 2.
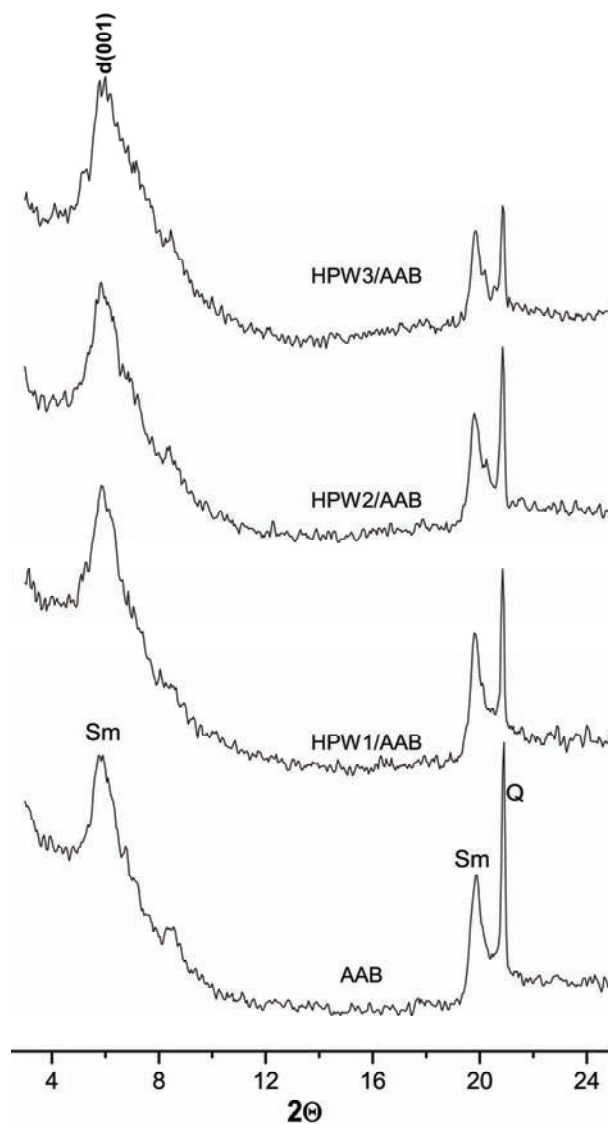

Figure 1. XRD Patterns of acid activated bentonite and HPW/AAB powders with various loading of 12-tungstophosphoric acid.

Table 1. Main crystallographic parameters measured on the (001) basal reflection of XRD patterns for acid activated bentonite and samples modified with various loading of HPW

Sample	Position 2θ CuK$_\alpha$, °	FWHM 2θ, °	Crystallite size nm
AAB	5.9	0.919	9.0
HPW1/AAB	5.9	1.135	7.3
HPW2/AAB	5.9	1.337	6.2
HPW3/AAB	5.9	1.693	4.9

The textural properties, specific surface area (S_{BET}), meso-external surface ($S_{m,e}$), average pore diameter (d), total pore volume (V_p) and micropore volume (V_{mic}) of the AAB and HPW/AAB powders are provided in Table 2.
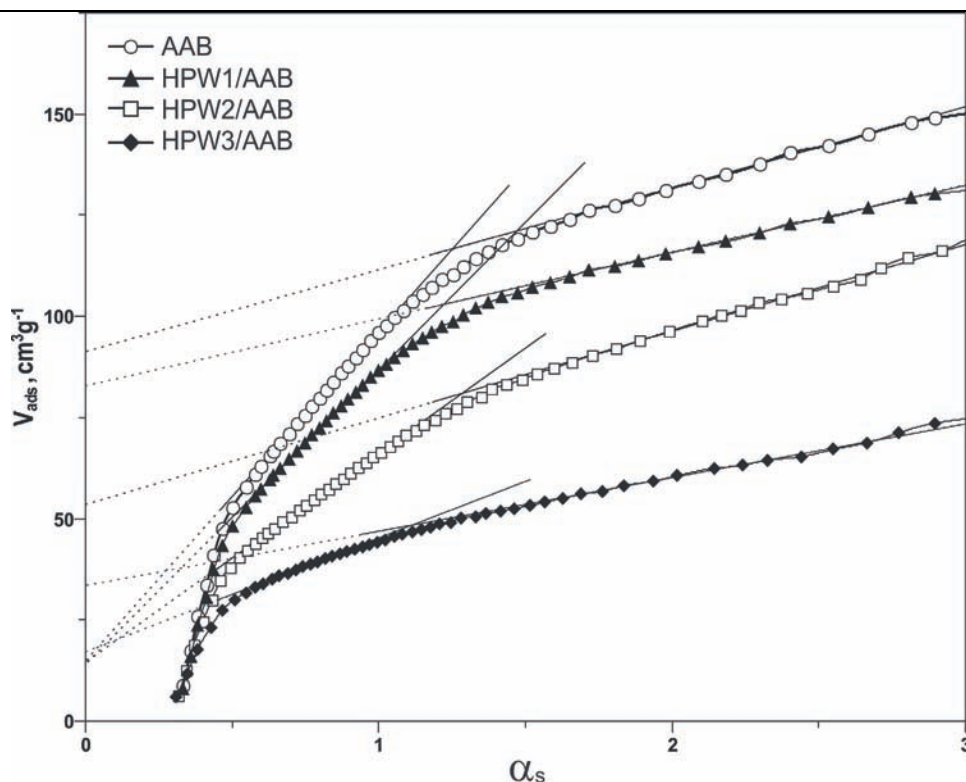
Figure 2. V_{ads} - α_s plots of acid activated bentonite and HPW/AAB powders with various loading of HPW.

Table 2. Pore structure parameters for acid activated bentonite and samples modified with various loading of HPW

Sample	S_{BET} $m^2 g^{-1}$	$S_{m,e}$ $m^2 g^{-1}$	d nm	$V_{0.98}$ $cm^3 g^{-1}$	V_{mic} $cm^3 g^{-1}$
AAB	272	256	3.65	0.242	0.118
HPW1/AAB	246	207	3.65	0.211	0.107
HPW2/AAB	188	175	3.62	0.195	0.081
HPW3/AAB	130	86	3.66	0.121	0.059

As shown in Table 2, among the samples with various loading of HPW, the sample HPW2/AAB maintains the smaller fraction of micropores and also the higher fraction of meso-external to BET surface area. The pure acid activated bentonite possesses the higher fraction of meso-external surface, coming mainly from the basal surface area of the bentonite particles. Lower values for the samples with various loading of HPW were observed. By using the data from adsorption isotherms, average pore diameter about 3.6 nm have been determined. The specific surface area was reduced at a high HPW loading due to the dispersion of HPW on the support. In other words, high HPW loadings reduced the accessibility of the pores of acid-activated bentonite to N_2. However, the mean pore diameter remained constant, indicating that the preparation procedure did not alter the primary structure of the support. Thus, only the partial

filling of pores was observed at high HPW loadings [29]. Since both, S_{BET} and V_p of the investigated samples decrease with HPW content, it can be concluded that electrocatalytic activity of samples toward nitrite ions does not arise from nitrite diffusion through the bentonite channels. The anionic electroactivity of HPW modified acid activated bentonites arise from interaction of nitrite ions with HPW.

To probe the morphological features of the AAB and HPW/AAB powders (Figure 3), the materials were observed by AFM.

Figure 3a clearly shows that the untreated samples is composed mainly of oriented domains of large rock blocks of about 1.5 μm in size, probably resulting from a preferable deposition of clay particles having a face-to-face interaction. The discontinuity in the film structure is evident by the presence of voids between the rock-blocks. On the acid-activated bentonite modified with various loading of HPW (Figures 3b-3d), a kind of preferable orientation is also preserved and the film presents a more textured and complex surface topography with a greater number of characteristics of lower size. However, a detailed analysis, Table 3, clearly demonstrated that the HPW//AAB powders present significantly higher fractal dimensions and lower roughness values than those of pure acid activated bentonite.
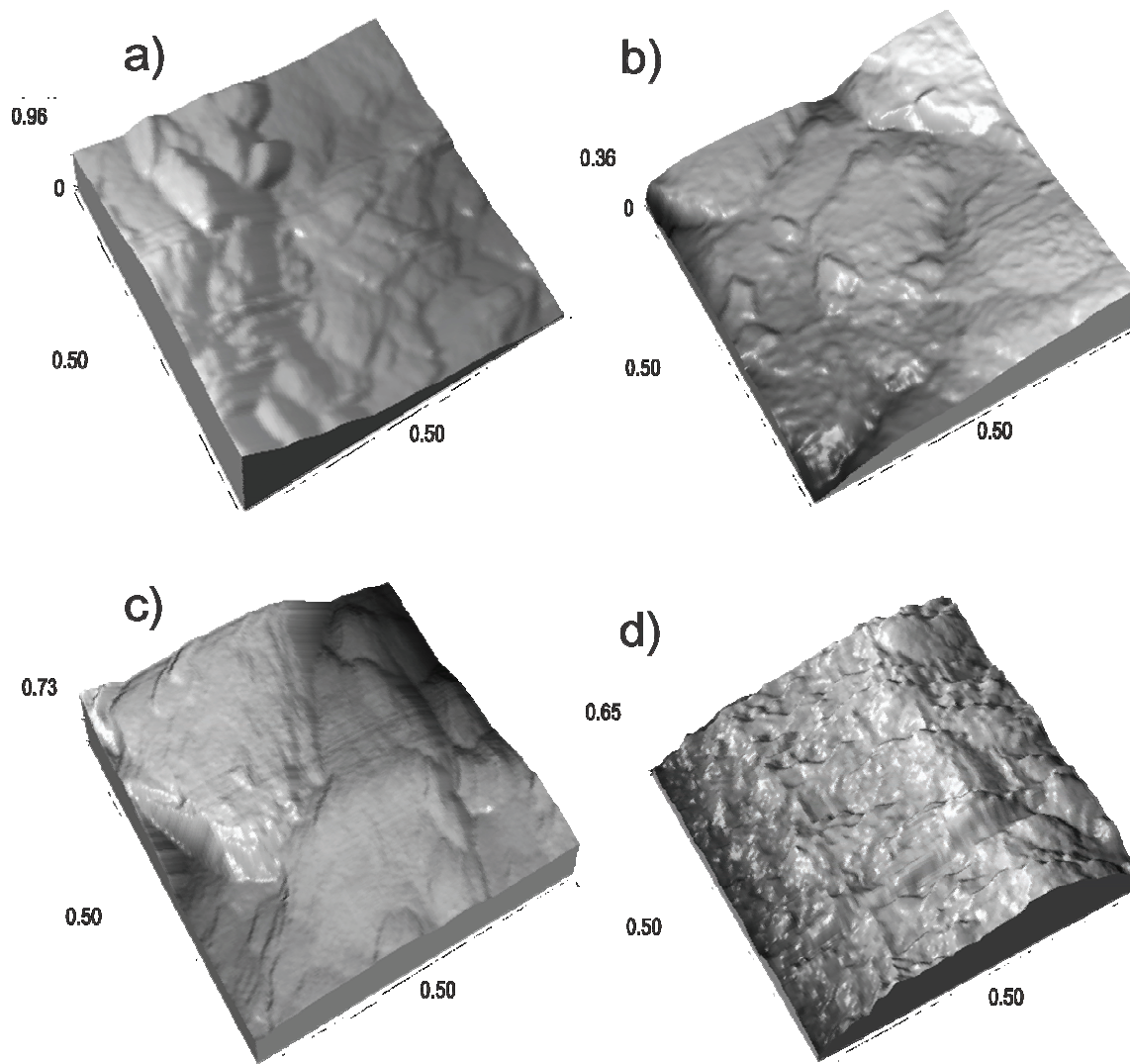
Figure 3. A three dimensional large-scale resolution AFM images of acid activated bentonite (a) and HPW/AAB powders with various loading of HPW (b, c and d).

Table 3. Fractal dimensions (D), RMS surface roughness, Rq, and average surface roughness, Ra, for acid activated bentonite and samples modified with various loading of HPW

Sample	Fractal dimension, D	Rq / nm	Ra / nm
AAB	2.55	480.3	387.5
HPW1/AAB	2.65	374.1	301.0
HPW2/AAB	2.62	285.1	223.6
HPW3/AAB	2.64	234.2	186.1

Characterization of the modified electrode

Cyclic voltammetry (CV) was employed to characterize the electrochemical properties of the AAB and HPW/AAB electrodes. Figure 4 shows the steady state cyclic voltammogram of thin film electrodes of acid activated bentonite a) and acid activated bentonites modified with various loading of HPW b) in 1 mM HCl + 1 M NaCl solution recorded at potential sweep rate of 50 mV s^{-1}. The steady state voltammograms of the investigated samples were obtained after 3-5 cycles with no significant difference beetwen voltamograms obtained in each cycle. Only 1HPW modified clay required 10-15 cycles to obtaine steady state CV. The peak currents decresed durring cycling until the constant value was obtained.

CV obtained for AAB electrode had no characteristic peaks in the potential range of -0.5 to 1.0 V. The cyclic voltammograms of HPW1/AAB and HPW2/AAB electrodes exhibited two peak couples, while HPW3/ /AAB voltammogram had three redox couples. In order to clarify the origin of the obtained peaks the cyclic voltammogram carbon glass electrode in supporting electrolyte containing 1 mM HPW solution is presented at the same Figure 4c.

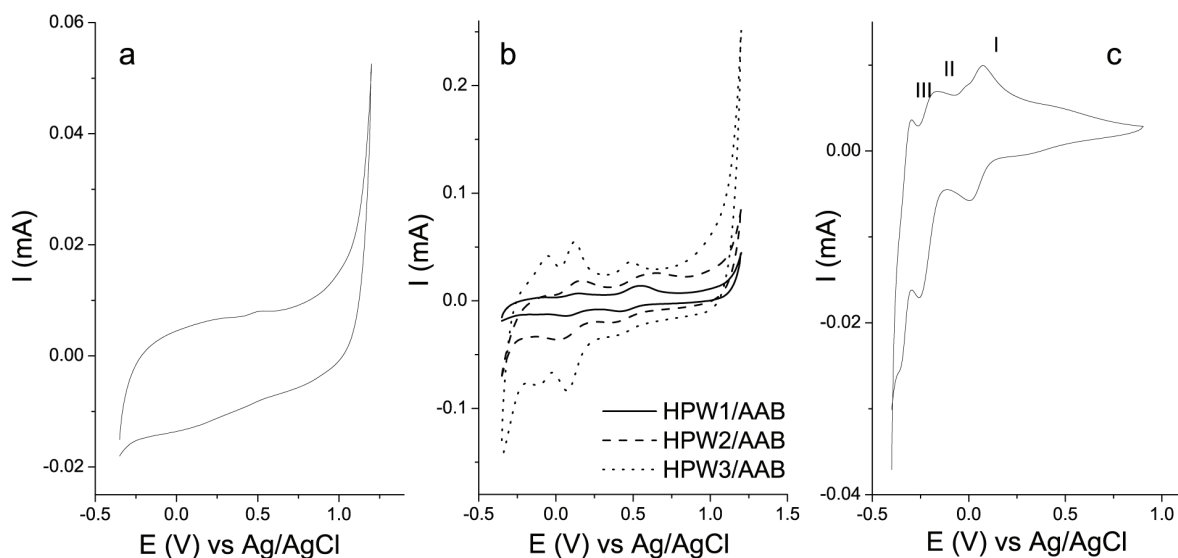At the cyclic voltammogram of the HPW solution three reversible redox peaks appeared (I, II and III in

333

Figure 4. Steady state cyclic voltammograms of thin film electrodes of acid activated bentonite (a) and acid activated bentonites modified with various loading of HPW (b) in 1 mM HCl + 1 M NaCl solution recorded at potential sweep rate of 50 mVs^{-1}. The cyclic voltammogram carbon glass electrode in supporting electrolyte containing 1mM HPW solution (c).

Figure 4c) with the mean peak potential, $E_{1/2}$, at 0.04, -0.21 and -0.33 V, respectively. Redox peaks I, II and III corresponded to reduction and oxidation of W through electron processes, which are nearly the same as those observed from the solution electrochemistry of PW$_{12}$ [30] and this behavior is characteristic for the HPW [31]. Both E_{pa} and E_{pc} were independent of the potential scan rates in the range of 10 to 400 mV s^{-1}. Each peak current was proportional to the square root of the scan rate indicating that the redox processes can be diffusion controlled processes.

At the resulting cyclic voltammogram of thin film electrodes (Figure 4b) all three redox peaks characteristic for HPW were obtained only for the thin film HPW3/AAB electrode. Both E_{pa} and E_{pc} were dependent of the potential scan rates in the range of 10 to 400 mV s^{-1}, although peak currents are proportional to the square root of the scan rate. This behavior indicated quasi-reversible nature of the investigated processes. The mean peak potentials, $E_{1/2}$, for HPW3/ /AAB were obtained at 0.40, 0.10 and -0.08 V, that are more positive potential values in comparison to the peak potentials obtained for HPW solution.

The electrocatalytic oxidation of nitrite at modified electrodes

The investigation of nitrite oxidation was performed after the steady-state voltammogram for electrode was obtained.

The oxidation of nitrite at the modified electrodes could be seen clearly in the 0.6 to 1.1 V range for all investigated electrodes, as shown in Figure 5a.

The increase of HPW content on the acid activated bentonite led to higher nitrite oxidation currents.

The results indicated that HPW3/AAB successfully decreased the overpotential of nitrite in comparison to carbon glass electrode (Figure 5b) and increased the catalytic current. This effect is probably caused by increased Brønsted acidity. It can be expected that addition of HPW to bentonite structure increase attraction of anions due to great number of OH groups in Keggin ion of HPW. Basically, increasing of Brønsted acidity of clay by adding HPW, might lead to enhancement of electrochemical activity [11].

Tafel slopes allows to conclude whether the rate-controlling step of the process is a first or a second electron transfer step and if a chemical reaction is involved. However, when porous electrodes are involved, additional potential drop in the pore is included. This potential drop is manifested as an increase of Tafel slope. The variation of the Tafel slop, b, with the concentration of NO$_2^-$ (Figure 6), from 180- -800 mV dec^{-1} for low W to 120-560 mV dec^{-1} for higher W can be interpreted by change of the mass transfer controlled region.

For HPW3/AAB electrode, Tafel slope of 120mV dec^{-1} was obtained for nitrite concentration of 2 mM, approaching the value of 118 mV dec^{-1} obtained for bare carbon glass electrode. Concentration gradient at high reactant concentration is low and potential drop in the pore is negligible, what makes porous electrode to behave as a flat electrode. This is in agreement with results obtained by Lasia [32].

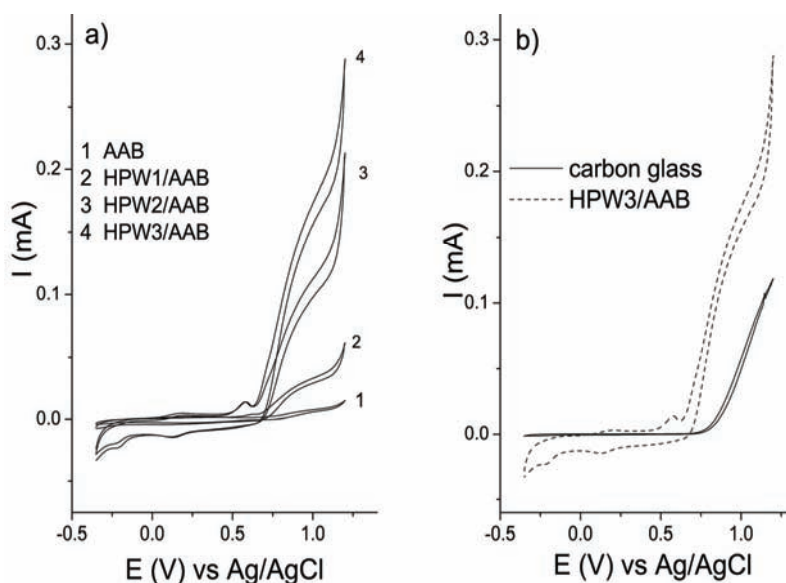Calibration plots for analysis of NO$_2^-$ show linear dependences of anodic peak current with increasing

Figure 5. Cyclic voltammograms of HPW/AAB electrodes in 2 mM $NaNO_2$ + 1 mM HCl + 1 M NaCl solution at potential sweep rate of 10 mV s^{-1} and rotation rate 600 rpm (a); b) comparison of CV curves for HPW3/AAB and bare glassy carbon electrodes.
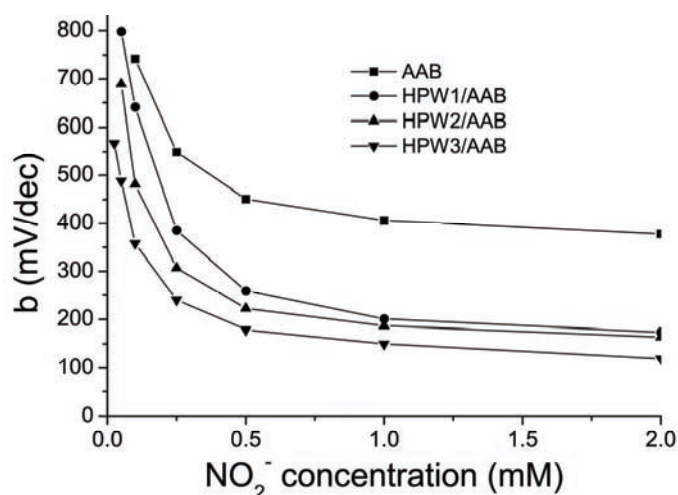

Figure 6. Dependence of Tafel slope of investigated HPW/AAB electrodes on nitrite ion concentration.

nitrite ions concentrations in the solution (Figure 7A) in the linear range of 0.025 to 2 mM and a correlation coefficient of 0.998.

The electrooxidation of nitrite on the AAB electrode gave low currents. The deviation of linear behavior at current vs. nitrite concentration plot was observed at upper end of the investigated concentration range (Figure 7B). HPW/AAB electrodes expressed higher nitrite oxidation currents than AAB electrode (Figures 8a-8c). The sensitivity of the modified electrodes of 12.9, 45.0 and 71.7 mA M^{-1} (HPW1/ /AAB, HPW2/AAB and HPW3/AAB respectively) was obtained.

A detection limit for modified electrodes, determined using a 3σ/slope ratio according to the IUPAC recommendations (Analytical Methods Committee,

1987) [33] was found to be 46, 13 and 8 µM for HPW1/AAB, HPW2/AAB and HPW3/AAB, respectively. Detection limit obtained for HPW/AAB electrodes is somewhat higher in comparison to detection limit obtained by other authors [34-36]. However, the sensitivity for HPW3/AAB is higher than sensitivity of other electrodes. The comparison of electroactivity with other materials is presented in Table 4.

Comparison of the nitrite response on HPW3/ /AAB electrode (Figure 8c), investigated with square wave voltammetry (SWV) and cyclic voltammetry (CV) showed that the sensitivity obtained by SWV are somewhat lower in comparison to those obtained by CV, although SWV is known to be more sensitive method.

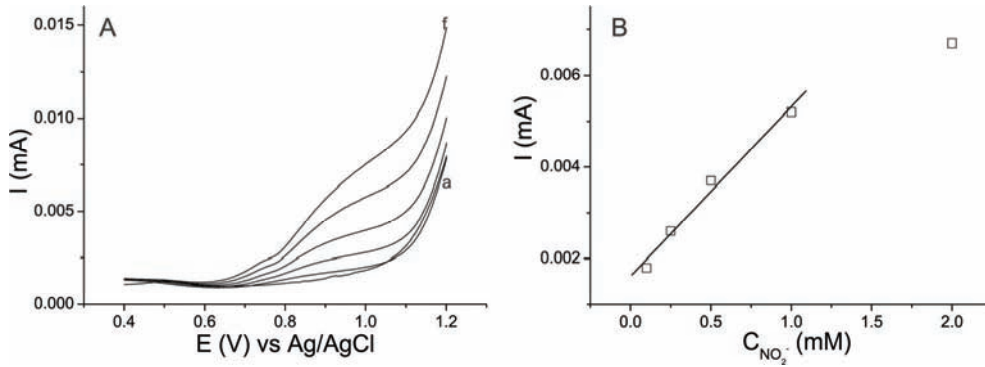The reproducibility of the HPW/AAB electrode for the nitrite determination was investigated. The nit-

Figure 7. A) Cyclic voltammogram of AAB electrode in 1 mM HCl + 1 M NaCl solutions containing NO_2^- in various concentrations a) 0, b) 0.1, c) 0.25, d) 0.5, e) 1 and f) 2 mM; potential sweep rate 50 mVs⁻¹. B) Calibration curve for NO_2^- at AAB electrode.
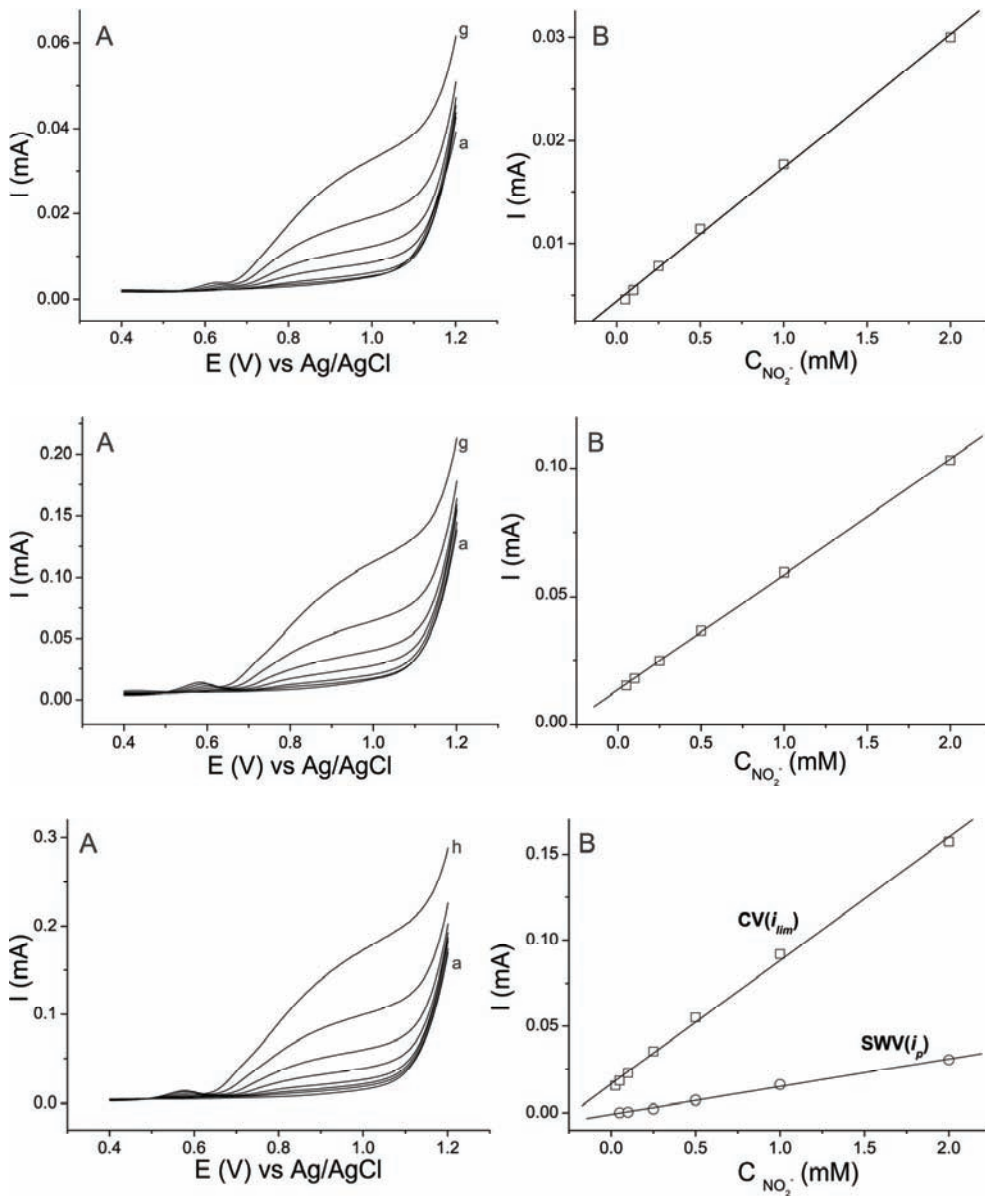

Figure 8. A) Cyclic voltammograms of HPW1/AAB, HPW2/AAB and HPW3/AAB electrodes (a, b and c, respectively) in 1 mM HCl + 1 M NaCl solutions containing NO_2^- in various concentrations a) 0, b) 0.05, c) 0.1, d) 0.25, e) 0.5 f) 1 and g) 2 mM.; potential sweep rate 50 mVs⁻¹. B) Calibration curves for NO_2^- at HPW1/AAB, HPW2/AAB and HPW3/AAB electrodes (a, b and c, respectively).

Table 4. Comparison of performances of different electrochemical sensors for nitrites

Electrode	Linear range, μM	Detection limit, μM	Sensitivity, mA M^{-1} cm^{-2}
H₃PMo₁₂O₄₀/PPy/MWCNTs-Au electrode [31]	5.0-34000	1.00	1214.1
GCE [32]	20-80	0.70	43.4
SPEBUME [33]	up to 3000	0.38	46.6×10^{-3}

rite detection was repeated three times on. Each time new electrode was applied on the carbon glass electrode and steady state voltammogram was obtained. The obtained calibration curves are presented at Figure 9.
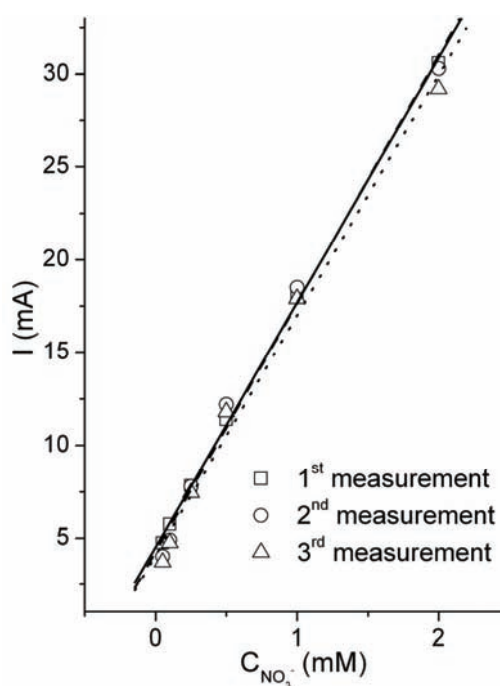

Figure 9. The calibration curves of three nitrite determination on HPW1/AAB electrode.

CONCLUSIONS

In this study, HPW/AAB powders with various loadings of HPW were synthesized. The resulting prepared powders showed mesoporous structure with a pore volume that varied according to the pore size in the range of 2-50 nm and value of crystallite size decrease with an increase in HPW loading. The electrochemical behavior of the HPW modified electrodes can be related to the physicochemical properties of the modifying materials. The observed differences between AAB and HPW/AAB samples were attributed to differences of structure, morphology and specific surface area of the corresponding bentonite powders. The prepared HPW/AAB electrode with the highest HPW loading showed enhanced electrocatalytic activity for oxidation of NO₂⁻ ions, which suggests that

electrode with high HPW loadings can serve as efficient sensor for nitrites oxidation reactions.

REFERENCES

[1]   E. Srasra, F. Bergaya, H. van Damme, N. K. Arguib, Appl. Clay Sci. **4** (1989) 411-421

[2]   G.E. Christidis, S. Kosiari, Clay Clay Miner. **51**(3) (2003) 327-333

[3]   Lj. Rožić, S. Petrović, T. Novaković, Russ. J. Phys. Chem. **83**(9) (2009) 1-4

[4]   Lj. Rožić, T. Novaković, S. Petrović, Z. Vuković. Ž. Čupić, Chem. Ind. Chem. Eng. Q. **14**(4) (2008) 227-229

[5]   P. Komadel, D. Schmidt, J. Madejevá, B.Cicel, Appl. Clay Sci. **5** (1990) 113-122

[6]   P. Falaras, F. Lezou, J. Electroanal. Chem. **455** (1998) 169-179

[7]   G.E. Christidis, A.E.Blum, D.D Eberl., Appl. Clay Sci. **34** (2006) 125-138

[8]   Lj Rožić., T. Novaković, S., Petrović, Appl. Clay Sci. **48** (2010) 154-158

[9]   M. Önal, Y. Sarikaya, Powder Technol. **172** (2007) 14-18

[10] D. Orata, F. Segor, React. Funct. Polym. **43** (2000) 305-314

[11] P. Falaras, F. Lezou, Ph. Pomonis, A. Ladavos, J. Electroanal. Chem. 486 (2000) 156-165.

[12] I. Tonle, E. Ngameni, A. Walcarius, Electrochim. Acta **49** (2004) 3435-3443

[13] M. Zhou, L.P. Guo, F.-Y. Lin, H.-X. Liu, Anal. Chim. Acta **587**(1) (2007) 124-131

[14] W. Sun, Y. Xian, H. Liu. W. Zhang, L. Jin, Fresenius J. Anal. Chem. **363** (1999) 236-240

[15] D. Ragupathy, A.I. Gopalan, K.-P. Lee, Microchim Acta **166**(3-4) (2009) 303-310

[16] T. McCormac, B. Fabre, G. Bidan, J. Electroanal. Chem. **427** (1997) 155-159

[17] Q. Tang, X. Luo, R. Wen, Anal. Lett. **38**(9) (2005) 1445-1456

[18] L. Liu, L. Tian, H. Xu, N. Lu, J. Electroanal. Chem. **587** (2006) 213-219

[19] G. Ranga Rao, B.G. Mishra, J. Porous Mater. **14**(2) (2007) 205-212

[20] S. Cosnier, S. Da Silva, D. Shan, K. Gorgy, Bioelectrochemistry **74**(1) (2008) 47-51

[21] M. Ammam, B. Keita, L. Nadjo, J. Fransaer, Talanta **80** (2010) 2132-2140

[22] R.J. Stanis, M.-C. Kuo, A.J. Rickett, J.A. Turner, A.M. Herring, Electrochim. Acta **53** (2008) 8277-8286

[23] M. Sadakane, E. Steckhan, Chem. Rev. **98** (1998) 219-238

[24] V.V. Bokade, G.D. Yadav, J. Nat. Gas Chem. **16** (2007) 186-192

[25] S.J. Gregg, K.S.W. Sing, Adsorption, Surface Area and Porosity, Academic Press, New York, 1982

[26] E.P. Barrett, L.G. Joyner, P.H. Halenda, J. Am. Chem. Soc. **73** (1951) 373-380

[27] Z. Mojović, P. Banković, A. Milutinović-Nikolić, B. Nedić, D. Jovanović, Appl. Clay Sci. **48** (2010) 179-184

[28] T. Novaković, Lj. Rožić, S. Petrović, A. Rosić, Chem. Eng. J. **137** (2008) 436-442

[29] Lj. Rožić, B. Grbić, N. Radić, S. Petrović, T. Novaković, Z. Vuković, Z. Nedić, Appl. Clay Sci. **53**(2) (2011) 151-156

[30] K. Unoura, N. Tanakz, Inorg. Chem. **22** (1983) 2963-2964

[31] W. Li, L. Li, Z. Wang, A. Cui, C. Sun, J. Zhao, Mater. Lett. **49** (2001) 228-234

[32] A. Lasia, J. Electroanal. Chem. **428** (1997) 155-164

[33] Analytical Methods Commitee, Analyst **112** (1987) 199--204

[34] Q. Tang, X. Luo, R. Wen, Anal. Lett. **38** (2005) 1445-1446

[35] E.H. Seymour, N.S. Lawrence, M. Pandurangappa, R. G. Compton, Microchim. Acta **140** (2002) 211-217

[36] J.-L. Chang, J.-M. Zen, Electroanal. **18**(10) (2006) 941--946.

ZORICA MOJOVIĆ[1]
LJILJANA ROŽIĆ[1]
TATJANA NOVAKOVIĆ[1]
ZORICA VUKOVIĆ[1]
SRDJAN PETROVIĆ[1]
DANIJELA RANĐELOVIĆ[2]
MIODRAG MITRIĆ[3]

[1]IHTM - Centar za katalizu i hemijsko inženjerstvo, Univerzitet u Beogradu, Beograd, Srbija
[2]IHTM - Centar za mikroelektronske tehnologije i kristale, Univerzitet u Beogradu, Beograd, Srbija
[3]Laboratorija za fiziku kondenzovane materije, Institut Vinča, Beograd, Srbija

NAUČNI RAD

ELEKTROHEMIJSKO PONAŠANJE PRAHA KISELO-AKTIVIRANOG BENTONITA MODIFIKOVANOG H₃PW₁₂O₄₀ KISELINOM

U ovom radu je analizirano elektrohemijsko ponašanje prahova kiselo-aktiviranog bentonita (AAB) modifikovanogsa 5, 10 i 20 mas.% 12-volframfosforne kiseline (HPW). Fizičkohemijske osobine pripremljenih prahova su određivane na osnovu analize snimljenih difraktograma praha, adsorpciono-desoprcionih izotermi azota, skenirajuće atomske mikroskopije (atomic force microscopy - AFM) i ciklovoltamograma. Rezultati AFM-a su pokazali da se prahovi uglavnom sastoje od orijentisanih domena velikih blokova, što je verovatno posledica povoljnije orijentacije čestica bentonita koje imaju bočnu interakciju. Takođe, je ustanovljeno da čestice modifikovanih uzoraka uglavnom imaju neuređenu mezoporoznu strukturu dok zapremina pora varira u skladu sa veličinom pora. Na osnovu difraktograma praha sintetisanih uzoraka izračunate su veličine kristalita i njihove vrednosti se nalaze između 4,9 i 9,0 nm. Elektrokatalitička aktivnost pripremljenih HPW/AAB elektroda je ispitana u reakciji oksidacije NO₂⁻ i rezultati su pokazali da ove electrode pokazuju veće struje oksidacije nitritnih jona nego AAB elektroda. Najbolja elektroaktivnost je uočena za HPW3/AAB elektrodu (AAB+20 mas.% HPW). Određeni limit detekcije (3σ) je iznosio 8 μM.

Ključne reči: elektrode od modifikovanog bentonita, fosforvolframska kiselina, oksidacija nitrita, ciklična voltametrija.